Monthly Notices
of the
ROYAL ASTRONOMICAL SOCIETY

MNRAS **480,** 5242–5259 (2018)
Advance Access publication 2018 August 13

doi:10.1093/mnras/sty2171

The GALAH survey and *Gaia* DR2: (non-)existence of five sparse high-latitude open clusters

Janez Kos,[1]★ Gayandhi de Silva,[1,2] Sven Buder,[3]† Joss Bland-Hawthorn,[1,4,5] Sanjib Sharma,[1] Martin Asplund,[4,6] Valentina D'Orazi,[7] Ly Duong,[6] Ken Freeman,[6] Geraint F. Lewis,[1] Jane Lin,[4,6] Karin Lind,[3,8] Sarah L. Martell,[3,9] Katharine J. Schlesinger,[6] Jeffrey D. Simpson,[9] Daniel B. Zucker,[10] Tomaž Zwitter,[11] Timothy R. Bedding,[1,13] Klemen Čotar,[11] Jonathan Horner,[12] Thomas Nordlander,[4,6] Denis Stello,[9,13] Yuan-Sen Ting[14,15,16] and Gregor Traven[11]

[1] *Sydney Institute for Astronomy, School of Physics A28, The University of Sydney, NSW 2006, Australia*
[2] *AAO-MQ, Macquarie University, Sydney 2109, Australia*
[3] *Max Planck Institute for Astronomy (MPIA), Koenigstuhl 17, D-69117 Heidelberg, Germany*
[4] *ARC Centre of Excellence for All Sky Astrophysics in 3 Dimensions (ASTRO-3D), Australia*
[5] *Sydney Astrophotonic Instrumentation Labs, School of Physics, A28, The University of Sydney, Camperdown, NSW 2006, Australia*
[6] *Research School of Astronomy & Astrophysics, Australian National University, Canberra, ACT 2611, Australia*
[7] *Istituto Nazionale di Astrofisica, Osservatorio Astronomico di Padova, vicolo dell'Osservatorio 5, I-35122, Padova, Italy*
[8] *Department of Physics and Astronomy, Uppsala University, Box 516, SE-751 20 Uppsala, Sweden*
[9] *School of Physics, UNSW, Sydney, NSW 2052, Australia*
[10] *Department of Physics and Astronomy, Macquarie University, Sydney, NSW 2109, Australia*
[11] *Faculty of Mathematics and Physics, University of Ljubljana, Jadranska 19, 1000 Ljubljana, Slovenia*
[12] *Division of Research and Innovation, University of Southern Queensland, Toowoomba, Queensland 4350, Australia*
[13] *Stellar Astrophysics Centre, Department of Physics and Astronomy, Aarhus University, DK-8000 Aarhus C, Denmark*
[14] *Institute for Advanced Study, Princeton, NJ 08540, USA*
[15] *Department of Astrophysical Sciences, Princeton University, Princeton, NJ 08544, USA*
[16] *Observatories of the Carnegie Institution of Washington, 813 Santa Barbara Street, Pasadena, CA 91101, USA*

Accepted 2018 August 7. Received 2018 August 03; in original form 2018 June 18

ABSTRACT

Sparse open clusters can be found at high galactic latitudes where loosely populated clusters are more easily detected against the lower stellar background. Because most star formation takes place in the thin disc, the observed population of clusters far from the Galactic plane is hard to explain. We combined spectral parameters from the GALAH survey with the *Gaia* DR2 catalogue to study the dynamics and chemistry of five old sparse high-latitude clusters in more detail. We find that four of them (NGC 1252, NGC 6994, NGC 7772, NGC 7826) – originally classified in 1888 – are not clusters but are instead chance projections on the sky. Member stars quoted in the literature for these four clusters are unrelated in our multidimensional physical parameter space; the quoted cluster properties in the literature are therefore meaningless. We confirm the existence of visually similar NGC 1901 for which we provide a probabilistic membership analysis. An overdensity in three spatial dimensions proves to be enough to reliably detect sparse clusters, but the whole six-dimensional space must be used to identify members with high confidence, as demonstrated in the case of NGC 1901.

Key words: techniques: radial velocities – catalogues – surveys – parallaxes – proper motions.

1 INTRODUCTION

The GALAH survey (De Silva et al. 2015; Buder et al. 2018) is a high-resolution ($R = 28\,000$), high signal-to-noise ratio (SNR ≈ 100) spectroscopic survey of one million stars. Its aim is to measure the abundances of up to 31 elements with a goal

★ E-mail: janez.kos@gmail.com
† Fellow of the International Max Planck Research School for Astronomy and Cosmic Physics at the University of Heidelberg, Germany.

to disentangle the chemical history of the Milky Way (Freeman & Bland-Hawthorn 2002). Observations specifically targeting open clusters are carried out as part of a dedicated programme (De Silva et al., in preparation) associated with the full GALAH survey. Such clusters play a fundamental role in our understanding of the chemical evolution of stars, since they are almost the only stellar population with homogeneous elemental abundances (De Silva et al. 2006, 2007; Sestito, Randich & Bragaglia 2007; Bovy 2016) arising from a common birth-time and place. Hence, processes in the evolution of stellar systems are best studied in clusters, including, but not limited to, the initial mass function of stars (Chabrier 2003; Krumholz 2014), the interaction with the disc (Gieles, Athanassoula & Portegies Zwart 2007; Gieles & Bastian 2008) or Galactic tidal fields (Baumgardt & Makino 2003), the creation of blue stragglers (Stryker 1993), initial binary fraction (Hurley, Aarseth & Shara 2007; Fregeau, Ivanova & Rasio 2009), radial migration (Fujii & Baba 2012), mass-loss (Miglio et al. 2012), and atomic diffusion (Bertelli Motta et al. 2018). Open clusters have long been considered as representatives of star formation in the Galaxy, because they are mostly found in the thin disc. Open clusters in other components of the Galaxy are rare, and so confirming their reality and measuring their properties is vital for using them to study the aforementioned processes in parts of the Galaxy outside the Galactic plane.

The clusters addressed in this work are generally believed to be old and far from the Galactic plane. At first glance, this is surprising because the survival time of such clusters is lower than their thin disc counterparts (Martinez-Medina et al. 2017). A simple model where most star formation happens in the thin disc has to be updated to explain open clusters at high galactic latitudes, assuming these are real.[1] The prevailing theories are heating of the disc (Gustafsson et al. 2016), soft lifting through resonances (Martinez-Medina et al. 2016), mergers (Kereš et al. 2005; Sancisi et al. 2008), and in situ formation from high-latitude molecular clouds (Camargo, Bica & Bonatto 2016). Sparse clusters are very suitable for testing the above theories because they are numerous and low in mass, and are therefore more likely to be involved in some of the above processes.

Sparse clusters are the last stage at which we can currently connect the related stars together before they dissipate into the Galaxy. Chemical tagging – the main objective of the GALAH survey – often uses such structures as a final test before attempting to tag field stars. Because sparse clusters are likely to be dissolving rapidly at the current epoch, we can expect to find many former members far from the cluster centre (de Silva et al. 2011; Kos et al. 2018). If these former members can be found, the dynamics of cluster dissipation and interaction with the Galactic potential could be studied in great detail.

Historically, sparse open clusters and open cluster remnants have been identified based on the aggregation of stars on the sky and their positions in the HR diagram. Spectroscopy has rarely been used, possibly because it was too expensive use of telescope time. Massive spectroscopic surveys either did not exist or only included one or a few potential members. Often, there was only one spectroscopically observed star in the cluster, so even for misidentified clusters the values for radial velocity (v_r) and metallicity[2] ([M/H], [Fe/H]) can

[1]Clusters can have high galactic latitude and still be well inside the thin disc if they are close to us. By high-latitude clusters, we mean those that are far from the Galactic plane.

[2]In the literature the metallicity [M/H] and iron abundance [Fe/H] are used interchangeably. We discuss the importance of differentiating between them in Section 3.

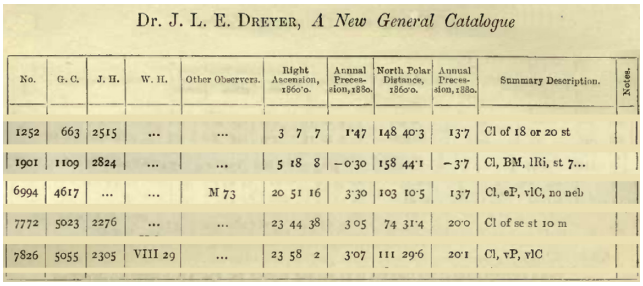

Dr. J. L. E. Dreyer, *A New General Catalogue*

No.	G. C.	J. H.	W. H.	Other Observers.	Right Ascension, 1860·0.	Annual Precession, 1880.	North Polar Distance, 1860·0.	Annual Precession, 1880.	Summary Description.	Notes.
1252	663	2515	...	...	3 7 7	1·47	148 40·3	13·7	Cl of 18 or 20 st	
1901	1109	2824	...	...	5 18 8	−0·30	158 44·1	−3·7	Cl, BM, IRi, st 7...	
6994	4617	...	...	M 73	20 51 16	3·30	103 10·5	13·7	Cl, eP, vlC, no neb	
7772	5023	2276	...	...	23 44 38	3·05	74 31·4	20·0	Cl of se st 10 m	
7826	5055	2305	VIII 29	...	23 58 2	3·07	111 29·6	20·1	Cl, vP, vlC	

Figure 1. For early observers these were without much doubt clusters of stars. The mistake could be attributed to '[...] accidental errors occasionally met with in the observations of the two HERSCHELS, and which naturally arose from the construction of their instruments and the haste with which the observations often necessarily were made.' (Dreyer 1888).

be found in the literature, even though the most basic spectroscopic inspection of a handful of stars would disprove the existence of the cluster. When identifying the clusters based on the position of stars in the HR diagram, most stars that fell close to the desired isochrone were used. Sparse clusters are often reported at high galactic latitudes, where the density of field stars is low and only a few are needed for an aggregation to stand out. Lacking other information, the phenomenon of pareidolia led early observers to conclude that many 'associations' were real (Fig. 1). The cluster labels have stuck, however, and several studies have been made of properties of these clusters (see Section 2.2 and references therein). It has happened before, that after more careful investigation that included proper motions and radial velocities, a cluster has been disproved (e.g. Han, Curtis & Wright 2016).

The amount of available data has increased enormously with *Gaia* DR2 (Gaia Collaboration 2018a). The search for new clusters will now be more reliable, given that precise proper motions and parallax add three more dimensions in which the membership can be established (Koposov, Belokurov & Torrealba 2017; Cantat-Gaudin et al. 2018; Castro-Ginard et al. 2018; Dias, Monteiro & Assafin 2018; Torrealba, Belokurov & Koposov 2018)

In Section 2 we review the studied data and explain the methods used to disprove the existence of four clusters and confirm a fifth. Section 3 provides more details about the analysis of the real cluster NGC 1901. In Section 4 we discuss some implications of our findings.

2 EXISTENCE OF CLUSTERS

2.1 Data

Stars observed as a part of the GALAH survey are selected from the 2MASS catalogue (Skrutskie et al. 2006). Depending on the observing mode, all the stars in a 1° radius field are in a magnitude range $12 < V < 14$ for regular fields and $9 < V < 12$ for bright fields; for full details on the survey selection process, and the manner in which observations are taken, we direct the interested reader to Martell et al. (2017) and Buder et al. (2018). See De Silva et al. (2015) for a formula to convert 2MASS photometry into V magnitudes. For some clusters targeted in the dedicated cluster program, we used a custom magnitude range to maximize the number of observed members. The V magnitude is calculated from the 2MASS photometry. In general, the GALAH V magnitude is ∼0.3 fainter than *Gaia* G magnitude.

Table 1. Coordinates of the clusters used in this work. For the non-existing clusters the heliocentric distances d and distances from the Galactic plane z are taken from the literature (see Section 2.2).

Cluster name	α °	δ °	l °	b °	d pc	z pc
NGC 1252	47.704	−57.767	274.084	−50.831	1000	−775
NGC 1901	79.490	−68.342	278.914	−33.644	426.0	−236.0
NGC 6994	314.750	−12.633	35.725	−33.954	620	−345
NGC 7772	357.942	16.247	102.739	−44.273	1500	−1050
NGC 7826	1.321	−20.692	61.875	−77.653	600	−590

Most of the data used in this work comes from the *Gaia* DR2 (Gaia Collaboration 2018a), which includes positions, G magnitudes, proper motions and parallaxes for more than 1.3 billion stars. This part of the catalogue is essentially complete for $12 < G < 17$, which is the range where we expect to find most of the cluster stars discussed in this paper. There are, however, a few members of the four alleged clusters that are brighter than $G = 12$ and are not included in *Gaia* DR2, but do not impact the results of this paper. We also disregarded all stars with the proper motion error >0.5 mas yr^{-1} or parallax error >10 per cent. Radial velocities in *Gaia* DR2 are only given for 7.2 million stars down to $G = 13$ (the limit depends on the temperature as well). Because the precision of radial velocities is significantly higher in the GALAH survey (Zwitter et al. 2018) than the *Gaia* data release, we use GALAH values wherever available. Because GALAH has a more limited magnitude range than *Gaia*, there are many stars for which *Gaia* DR2 radial velocities must be used. From the cluster stars used in this work that have radial velocity measured in both *Gaia* DR2 and GALAH we find no systematic differences larger than 0.2 km s^{-1} between the two surveys, so we can use whichever velocity is available.

2.2 Clusters

In the fields observed by the GALAH survey, we identified 39 clusters with literature references. Four of them (NGC 1252, NGC 6994, NGC 7772, and NGC 7826) appeared to have no observed members – stars clumped in the parameter space – even though we targeted them based on the data in the literature. All four clusters are sparse (with possibly only ∼10 members), are extended, and at high galactic latitudes. Among the other 35 observed clusters we only found one (NGC 1901) that is morphologically similar to those four and appears to be a real open cluster. We observed more clusters at high latitudes (Blanco 1, NGC 2632, M 67, and NGC 817), but they are all more populated than the five clusters studied here. See Table 1 for a list of basic parameters of these five clusters, and the summary below:

(i) NGC 1252 was thought to be metal poor, old (3 Gyr), and far from the Galactic plane ($z = -900$ pc). This would be a unique object, as no such old clusters are found that far from the plane (de la Fuente Marcos et al. 2013). It has been argued in the past that this cluster is not real (Baumgardt & Makino 2003).

(ii) NGC 1901 is most probably a real open cluster, as confirmed by the literature (Eggen 1996; Pavani et al. 2001; Dias et al. 2002; Carraro et al. 2007; Kharchenko et al. 2013; Conrad et al. 2014) and our own observations. In the literature NGC 1901 is younger (400 Myr) and closer (360 pc) than the other four objects discussed here (Carraro et al. 2007). See Section 3 for our own analysis of this cluster.

(iii) NGC 6994 was thought to be old (2–3Gyr), relatively far away from the plane ($z = -350$ pc) and a dynamically well evolved cluster remnant (Bassino, Waldhausen & Martínez 2000). Carraro (2000) and Odenkirchen & Soubiran (2002) successfully argue that NGC 6994 is neither a cluster or a remnant, but only an incidental overdensity of a handful of stars.

(iv) NGC 7772 was thought to be 1.5 Gyr old, more than 1 kpc below the plane and depleted of low mass stars (Carraro 2002).

(v) NGC 7826 has never been studied in detail. It is included in some open cluster catalogues (Dias et al. 2014), in which an age of 2 Gyr and a distance from the Galactic plane of $z = -600$ pc are assumed.

2.3 Literature members

In Tables A1–A4 we review the available memberships from the literature for clusters NGC 1252, NGC 6994, NGC 7772, and NGC 7826. It is clear they are not clusters and the possible members are in no way related, based on the *Gaia* DR2 parameters and occasionally GALAH radial velocities. We cross matched the lists of members given in the literature to *Gaia* DR2 targets based on positions and magnitude, so all the parameters given in Tables A1–A4 are from *Gaia* DR2 or GALAH. After the tables we also show HR diagrams using literature members and their *Gaia* DR2 magnitudes (Figs A1–A4). A small fraction of members in the literature cannot be cross-matched with *Gaia* DR2, either because the star is absent from *Gaia* DR2, the coordinates in the literature are invalid, or the members are not clearly marked in a figure or table.

In contrast to our findings for the four other clusters, our results confirm that NGC 1901 is a real cluster, and provide our own membership analysis in Section 3.

2.4 6D parameter space

Figs 2 and 3 show the six-dimensional space (α, δ, μ_α, μ_δ, ϖ, v_r) for all five clusters. We choose to display observed parameters for various reasons; their uncertainties are mostly Gaussian and independent, which cannot be said for derived parameters [actions, orbital parameters, (U, V, W) velocities, etc.], and when the radial velocity is not available we can still use the remaining five parameters. Also, a cluster is a hyperellipsoid in both observed and any derived space, so nothing can be gained from coordinate transformations. There is no common definition of a cluster (or a cluster remnant), but it makes sense that a necessary condition is that the cluster members form an overdensity in space, regardless of the dynamics of the cluster. This is another reason why measurables should be used, because they are already separated into three spatial dimensions and three velocities. In each figure we plot positions of stars on the sky (α, δ) in the left-hand panel, while proper motions are plotted in the middle panel and the final two measurables (ϖ and v_r) are plotted in the right-hand panel.

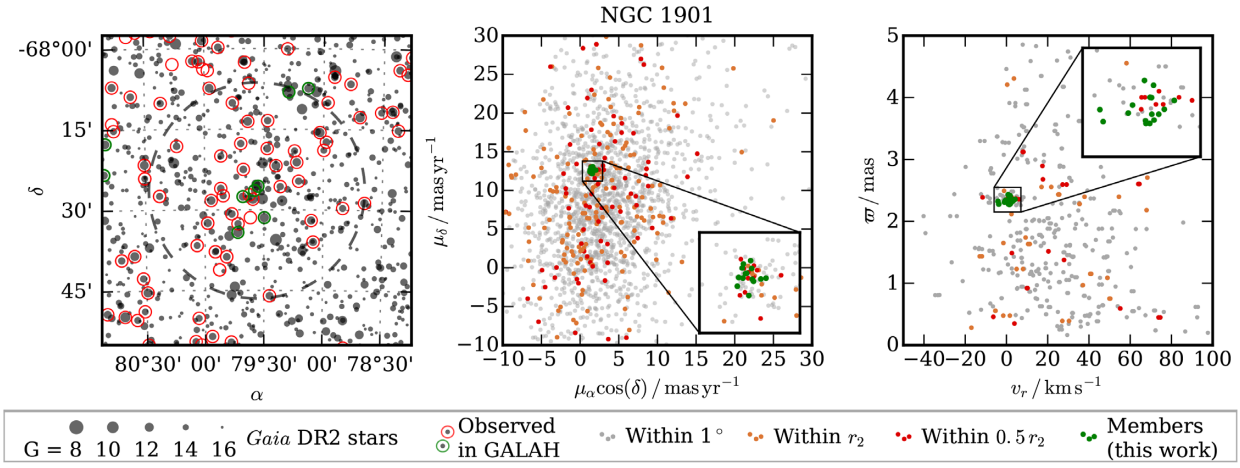

Figure 2. Six-dimensional space for stars in and around NGC 1901. Left: Position of *Gaia* DR2 stars with magnitude $G < 16$ (grey) with marked members observed in the GALAH survey (circled in green) and other stars observed in GALAH (circled in red). The dashed circle marks the cluster radius r_2. Middle: *Gaia* DR2 proper motions for all stars inside a 1° radius from the cluster centre (grey), stars inside r_2 (orange), stars inside $0.5\,r_2$ (red), and identified members (green). Right: Radial velocity and parallaxes for stars that have radial velocity measured either in *Gaia* DR2 or in the GALAH survey. Same colours are used as in the middle panel.

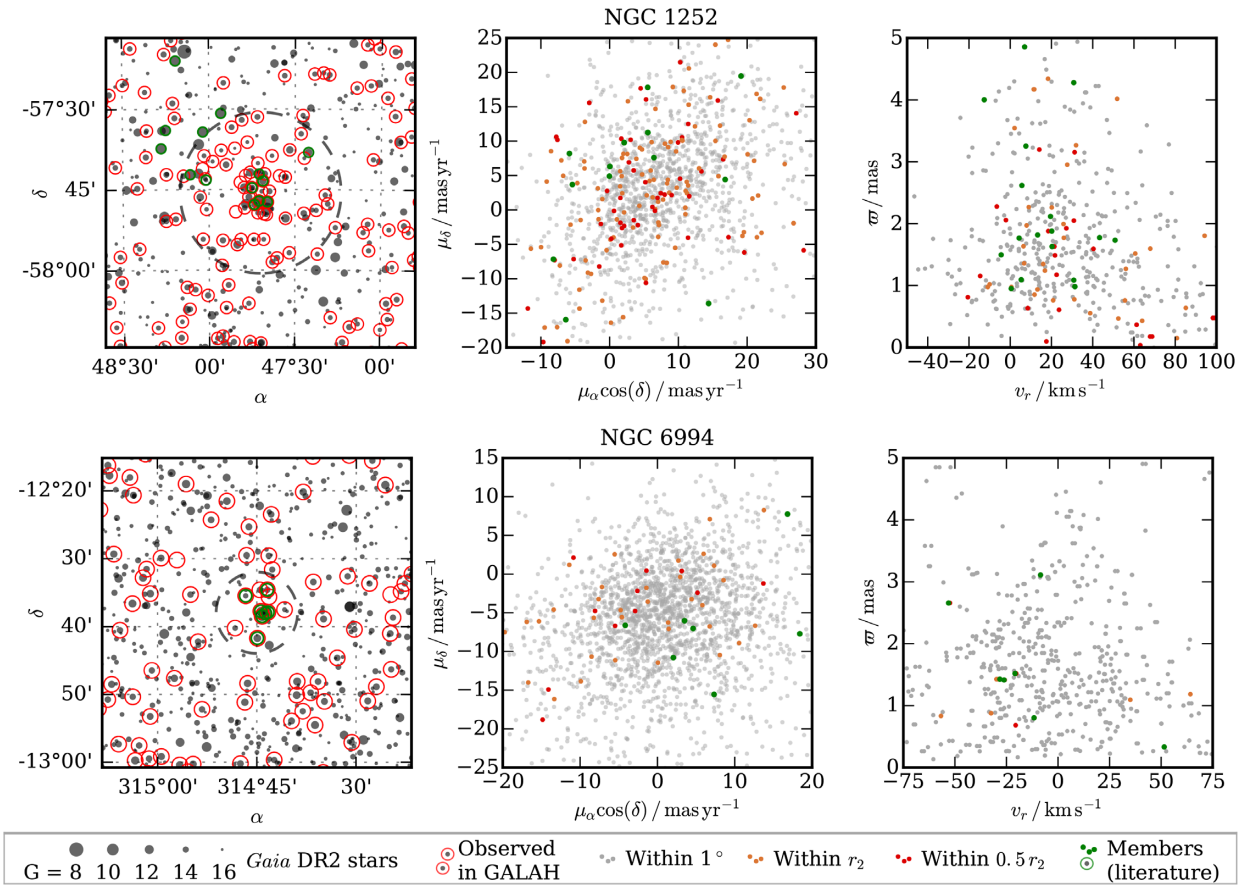

Figure 3. Six-dimensional space for stars in and around NGC 1252 (top row) and NGC 6994 (bottom row). Left: Position of *Gaia* DR2 stars with magnitude $G < 16$ (grey) with marked stars observed in the GALAH survey (circled in red) and faux members from the literature (circled in green). The dashed circle marks the cluster radius. Middle: *Gaia* DR2 proper motions for all stars inside a 1° radius from the cluster centre (grey), stars inside r_2 (orange), stars inside $0.5\,r_2$ (red), and faux members from the literature (green). Right: Radial velocity and parallaxes for stars that have radial velocity measured either in *Gaia* DR2 or in the GALAH survey. Same colours are used as in the middle panel.

For NGC 1901 in Fig. 2, we clearly see clumping in both the proper-motion plane and the parallax-radial-velocity plane. An overdensity in all three spatial dimensions for this cluster is illustrated in Fig. 4. The overdensity, however, is not obvious in the

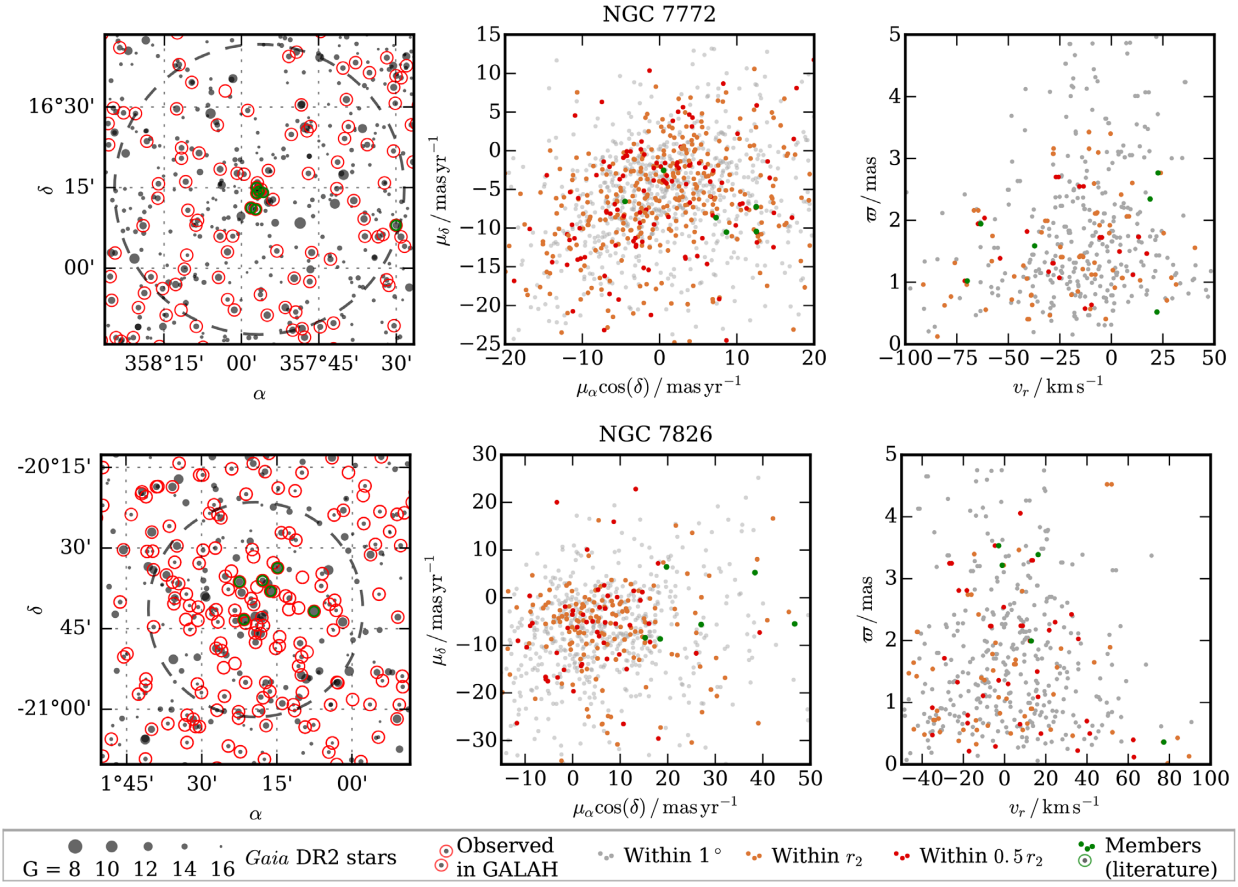

Figure 3. *–continued*

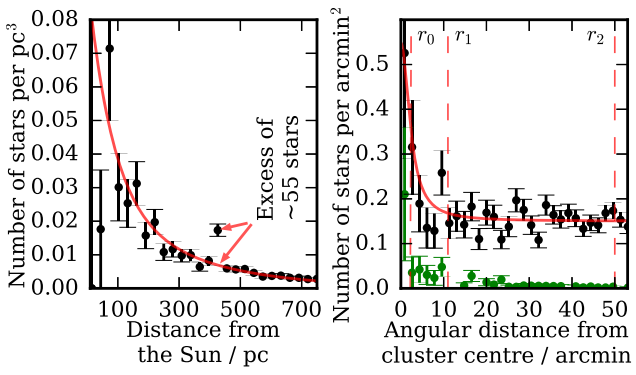

Figure 4. Left: Density of stars as a function of distance from the Sun in the direction of NGC 1901. NGC 1901 produces a very significant (5σ) signal at 426 pc. Stars in a 1° cone around the cluster centre are used for this plot. Right: Star density as a function of apparent distance from NGC 1901 centre. An overdensity above the background level (0.15 stars per arcmin^2) is clearly detected. Black points show measurements for all stars with magnitude $G <$ 17 and green points only show the density of the most probable members. Eyeballed radii r_0, r_1, and r_2 as defined in Kharchenko et al. (2012) are marked. Red curve is a fitted King model.

(α, δ) plane. One would expect a similar clumping for the other four clusters, if they were real. Instead, as seen in Fig. 3, we cannot find a single pair of stars (either among the literature members or all *Gaia* stars), that are close together in all six dimensions, even though the overdensity in (α, δ) appears similar to that of NGC 1901.

3 NGC 1901 ANALYSIS

Since NGC 1901 is a real cluster, we provide here our own membership analysis. First, we performed a vague cut in the 6D space ($r < 0.5°$, 0.7 mas yr^{-1} $< \mu_\alpha <$ 2.5 mas yr^{-1}, 11.7 mas yr^{-1} $< \mu_\delta <$ 13.5 mas yr^{-1}, 1.8 mas $< \varpi <$ 2.8 mas, and -2.0 km s^{-1} $< v_r <$ 7.0 km s^{-1}) to isolate the most probable members. This yielded 80 stars, of which 20 have radial velocities. Most of these stars are members, therefore the mean position of these stars in the six-dimensional space is very close to the mean position of the cluster. We therefore used these stars to estimate the mean and spread in every dimension independently (there seems to be no correlation between different dimensions/parameters), which we used to perform a probability analysis. The probability for a star with given parameters (α, δ, μ_α, μ_δ, ϖ, and v_r) to be a member is described by a multivariate Gaussian centred on the mean values obtained by a vague cut. For stars with existing radial velocity measurement we produce two probabilities, one with radial velocity taken into account (P_{6D}) and one without it (P_{5D}). From the difference between these, we estimate that ~15 per cent of highly probable members based only on the 5D analysis would have their probability reduced significantly if the radial velocity measurements were available. Membership probabilities are given in Table B1 as well as an indication of possibly binaries based on GALAH spectra. Re-fitting the multivariate Gaussian based on the improved membership probabilities changes the probabilities insignificantly and does not impact the rank of the most probable members.

From the most probable members we can calculate the mean parameters of NGC 1901, along with their uncertainties. Weighted

means and standard deviations are calculated only from the stars in Table B1, using P_{5D} as the weight or P_{6D}, where available. The exceptions are cluster radii, iron abundance, alpha elements abundance, and age, which are all calculated from the members with $P_{5D} > 0.4$ and $P_{6D} > 0.4$, where available. The following parameters are given in Table 2. Positions α, δ and l, b give the cluster centre in celestial and galactic coordinates, respectively. Radii r_0, r_1, and r_2 are estimated visually as described in Kharchenko et al. (2012). r_0 corresponds to the core radius, where the radial density profile falls sharply. At r_1 the density stops abruptly and at r_2 it becomes indistinguishable from the density of the surrounding field. King's (King 1962) core radius (r_c) and tidal radius (r_t) are fitted, although we were unable to measure the tidal radius with any meaningful confidence. Proper motions, μ_α and μ_δ, are the mean values for the cluster and the uncertainties relate to the mean, not to the dispersion. The radial velocity (v_r) and the velocity dispersion (σ_{v_r}) are measured from a combination of *Gaia* DR2 and GALAH radial velocities. The distance (dist.) is calculated from the parallaxes (ϖ). A normal distribution for the parallax of each star was sampled and the distance calculated for every sample. The reported distance and its uncertainty are the mean and standard deviation of all the samples for all members. Distance uncertainty might be underestimated, if the parallaxes of individual stars have correlated errors.

Iron and α abundances ([Fe/H], [α/Fe]) are calculated by SME (Valenti & Piskunov 1996; Piskunov & Valenti 2017) from the GALAH spectra in the same manner as in Buder et al. (2018) and are based on eight members only. Other members observed in GALAH are too hot for a consistent analysis. Measured metallicities, as well as abundances of other elements are in Table C1. Age (log t) is calculated by isochrone fitting. Of the individual elements, we highlight that the cluster displays high Ba abundance of over 0.4 dex, while the Y abundances are closer to Solar values. High Ba abundances in young open clusters seem to be correlated with cluster age (D'Orazi et al. 2009). However why other s-process element abundances such as Y are not similarly enhanced remains an outstanding issue in open cluster literature (D'Orazi, De Silva & Melo 2017).

Putting the most probable members on to the colour–magnitude diagram (Fig. 5) and fitting Padova isochrones (Marigo et al. 2017) allows us to measure the age of the cluster. The precision of the calculated age is somewhat limited, as there are only a few stars close to the turn-off point. The reddening and colour excess as measured by *Gaia* are higher than the literature values and the correlations between the age and reddening/extinction can increase the age uncertainty even further. From fitting the isochrones, we can also tell that there is a significant difference between the metallicity ([M/H] $= -0.13$) of the best-matching isochrone and the iron abundance ([Fe/H] $= -0.27$) we measured in the GALAH survey. This mismatch is due to the difference between the two quantities. We also measured the abundance of other elements and they are close to or above solar values. Using a formula from Salaris, Chieffi & Straniero (1993) to combine iron abundance and alpha elements abundance into metallicity:

$$\left[\frac{\mathrm{M}}{\mathrm{H}}\right] = \left[\frac{\mathrm{Fe}}{\mathrm{H}}\right] + \log\left(0.638 \cdot 10^{[\alpha/\mathrm{H}]} + 0.362\right), \quad (1)$$

we get a value [M/H] $= -0.15$, which is consistent with the photometrically obtained metallicity. Both the metallicity and iron abundance are lower than the numbers quoted in the literature ([Fe/H] $= -0.08 \pm 0.02$). The latter is based on a single measurement of HD 35294, which might not be a member of NGC 1901,

Table 2. Final parameters for NGC 1901. Measurement uncertainties are given after the ± sign in the bottom row.

α	δ	l	b	r_0	r_1	r_2	r_c	r_t	$\mu_\alpha \cos(\delta)$	μ_δ	v_r	ϖ	dist.	σ_{v_r}	$\left[\frac{\mathrm{Fe}}{\mathrm{H}}\right]$	$\left[\frac{\alpha}{\mathrm{Fe}}\right]$	log t
°	°	°	°	arcsec	arcsec	arcsec	arcsec	arcsec	mas y^{-1}	mas y^{-1}	km s^{-1}	mas	pc	km s^{-1}	dex	dex	log yr
79.490	−68.342	278.914	−33.644	2.2	11.0	50.0	2.4	>20	1.632	12.671	1.30	2.349	426.0	2.80	−0.27	0.07	8.84
±0.106	±0.031	±0.039	±0.043	±0.5	±2.5	±12.0	±0.7		±0.030	±0.018	±0.28	±0.009	±2.0	±0.27	±0.05	±0.05	±0.05

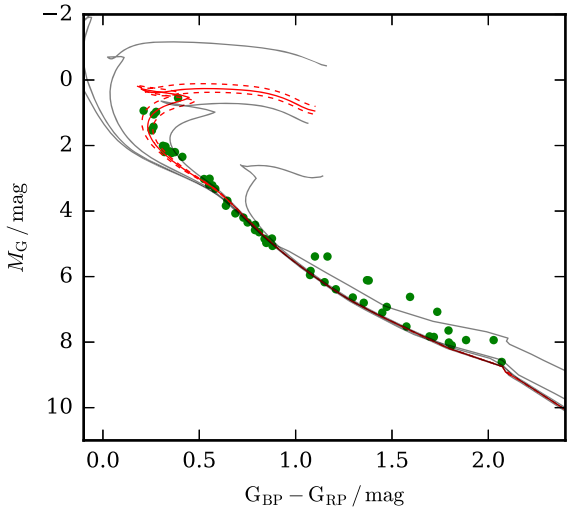

Figure 5. NGC 1901 members on the colour–magnitude diagram. Padova isochrones (Marigo et al. 2017) are plotted for log $t = 8.84$ (red solid curve, 692 Myr), and for log $t = 8.80$ and log $t = 8.88$ (red dashed curves), all with [M/H] $= -0.13$. Instead of using unreliable extinctions and reddenings for individual stars, an extinction of $A_V = 0.27$ was used and we assumed $R_V = 3.1$. Isochrones for log $t = 8.0$, 8.5, 9.0, and 9.5 are also plotted in grey. Varying the membership probability cut-off within reasonable values does not add or remove any turn-off stars.

as it has a parallax of 1.49 ± 0.03 mas, much less than the mean of the cluster.

NGC 1901 has been referred to as an open cluster remnant in the literature (e.g. by Carraro et al. 2007). While there is no clear consensus on the classification of an open cluster remnant, if an open cluster is sparsely populated with more than two-thirds of its initial stellar members lost, then a cluster like NGC 1901 is classed as a cluster remnant (Bica et al. 2001). However, as NGC 1901 appears to be a rapidly dissolving cluster (as is evident from a large velocity dispersion and being labelled as a remnant in the literature), it is not expected to survive another pass through the Galactic plane in around 18 Myr time (the last time it passed the Galactic plane was 26 Myr ago). We used *galpy*[3] (Bovy 2015) to calculate the orbit of individual stars in the cluster. Currently, the velocity dispersion of the cluster is 2.8 km s^{-1}. By the time the cluster passes through the Galactic plane, the members will be spread out in a diameter ∼7 times larger than they are now. This is enough that the cluster will be undetectable with the approach used in this paper.

Eggen (1996) referred to the NGC 1901 'supercluster', comprising a co-moving group of unbound stars associated with the cluster. The NGC 1901 supercluster has been proposed to be dynamically related to the Hyades supercluster (the unbound group of stars co-moving with the Hyades open cluster), due to the similar space motions of the two groups (Dehnen 1998), and they are jointly referred to as Star Stream I by Eggen (1996). While the detection of the extended members of the NGC 1901 supercluster is beyond the scope of this paper, it is certainly plausible that the dispersed members of NGC 1901 are detectable within the Galactic motion space and could be used to gain insights into the dispersion mechanisms of the cluster.

[3] http://github.com/jobovy/galpy

4 DISCUSSION

Clusters cannot be simply split into high- and low-latitude, or sparse and rich clusters. There are a range of factors that could be specific to each cluster, depending on its initial mass, origin and evolutionary history. Furthermore, with typical cluster dispersion processes the transition is smooth and there are other clusters similar to the ones described in this paper among the 39 clusters in our data set, such as Blanco 1 and NGC 1817. We chose not to include such clusters here because they are slightly more populated and lie closer to the Galactic plane than the clusters discussed above. Also, the cluster sample in our data set was not observed with a clear selection function, apart from trying to cover as wide range of ages and metallicities as possible. As a result, it would not be reasonable to extrapolate from the results presented in this work to conclude that four out of five sparse high-latitude clusters are not real. However, a lesson learned is that the existence of sparse clusters should be double-checked, regardless of how reputable the respective cluster catalogues are. Surveys of high-latitude clusters (Bica et al. 2001; Schmeja et al. 2014), after the *Gaia* parameters are included, will probably give a better picture.

It is expected that some sparse clusters are not real. The rate of faux clusters can be estimated from mean star densities and the number of possible members in the aggregation. Fig. 6 shows the probability as a function of the galactic latitude (a proxy for background star density) and the number of stars in the aggregation. We estimated the number of members of the four faux clusters from literature sources. The background star density is calculated from *Gaia* DR2. All four faux clusters lie in the region where low-probability clusters are expected to be found.

An overall existence probability of a cluster could be calculated in the same way we calculate membership probabilities in NGC 1901. Instead of probabilities for individual stars the distribution of suspected members could be compared to a plausible multivariate Gaussian and a single number for the existence probability of the cluster could be reported. It is evident from Fig. 3 that such probability would be essentially zero for the four disproved clusters.

For NGC 1901 we found more members than one would find using the same literature as for the four faux clusters, so the position of NGC 1901 on plots in Fig. 6 with respect to the faux clusters might not be completely representative. NGC 1901 also lies in front of the LMC, so the background count in the $G < 16$ panel is underestimated.

We can conclude that existence of the four false clusters has never been very plausible, since they were all discovered based on the star counts only. Most probably, there are more long-known sparse clusters that will be disproved in the near future.

Gaia parameters are obviously proving to be well suited for cluster membership analysis, as well as for finding new clusters (Koposov et al. 2017; Cantat-Gaudin et al. 2018; Castro-Ginard et al. 2018; Dias et al. 2018; Torrealba et al. 2018). The fraction of reported clusters that are not real will probably be significantly less than in the past, but even in the *Gaia* era we can expect to find low-probability clusters that should be treated with caution. The same holds for membership probabilities. We show that positions, proper motions, and distances are not enough and the whole 6D information must be used to find members with great certainty.

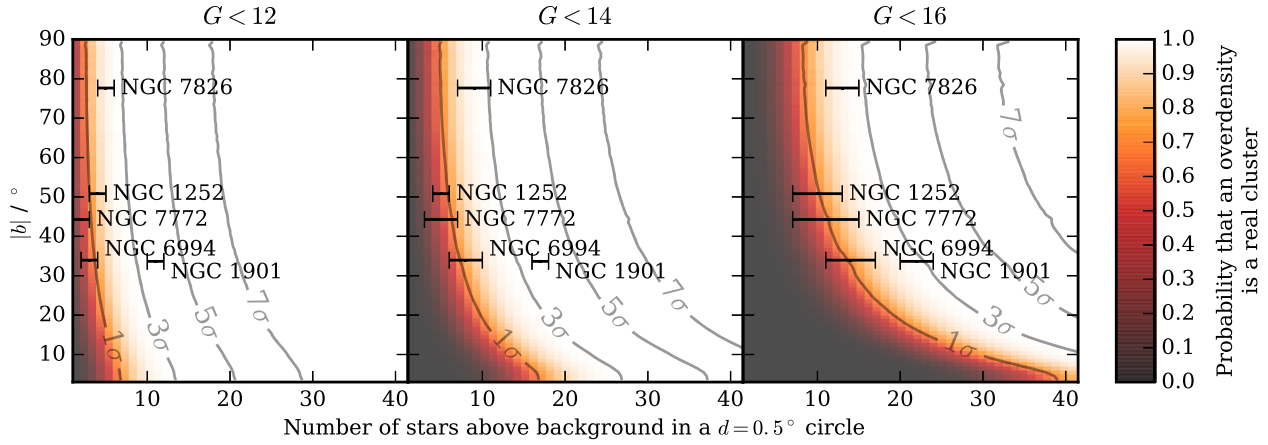

Figure 6. Probability that an overdensity of N stars above the background level in a 0.5° diameter circle is a real cluster. Panels show the probability for different magnitude cuts between $G < 12$ (left) and $G < 16$ (right). The probability changes significantly with the background level. Here we only show the variation as a function of absolute galactic latitude ($|b|$). Only minor differences in local density can be expected for regions around different clusters. Position of clusters studied in our work is indicated. For the non-existent clusters we estimated the supposed number of stars from the literature sources. For all five clusters we assumed a radius of 0.25°, so all of them can be shown on the same plot.

ACKNOWLEDGEMENTS

JK is supported by a Discovery Project grant from the Australian Research Council (DP150104667) awarded to J. Bland-Hawthorn and T. Bedding. SB acknowledges funds from the Alexander von Humboldt Foundation in the framework of the Sofja Kovalevskaja Award endowed by the Federal Ministry of Education and Research. SLM acknowledges support from the Australian Research Council through grant DP180101791. Parts of this research were conducted by the Australian Research Council Centre of Excellence for All Sky Astrophysics in Three Dimensions (ASTRO 3D), through project number CE170100013. GT, KČ, and TZ acknowledge the financial support from the Slovenian Research Agency (research core funding No. P1-0188).

REFERENCES

Bassino L. P., Waldhausen S., Martínez R. E., 2000, A&A, 355, 138
Baumgardt H., Makino J., 2003, MNRAS, 340, 227
Bertelli Motta C. et al., 2018, MNRAS, 478, 425
Bica E., Santiago B. X., Dutra C. M., Dottori H., de Oliveira M. R., Pavani D., 2001, A&A, 366, 827
Bouchet P., The P. S., 1983, PASP, 95, 474
Bovy J., 2015, ApJS, 216, 29
Bovy J., 2016, ApJ, 817, 49
Buder S. et al., 2018, MNRAS, 478, 4513
Camargo D., Bica E., Bonatto C., 2016, A&A, 593, A95
Cantat-Gaudin T. et al., 2018, preprint (arXiv:1805.08726)
Carraro G., 2000, A&A, 357, 145
Carraro G., 2002, A&A, 385, 471
Carraro G., de La Fuente Marcos R., Villanova S., Moni Bidin C., de La Fuente Marcos C., Baumgardt H., Solivella G., 2007, A&A, 466, 931
Castro-Ginard A., Jordi C., Luri X., Julbe F., Morvan M., Balaguer-Núñez L., Cantat-Gaudin T., 2018, preprint (arXiv:1805.03045)
Chabrier G., 2003, PASP, 115, 763
Conrad C. et al., 2014, A&A, 562, A54
D'Orazi V., Magrini L., Randich S., Galli D., Busso M., Sestito P., 2009, ApJ, 693, L31
D'Orazi V., De Silva G. M., Melo C. F. H., 2017, A&A, 598, A86
de la Fuente Marcos R., de la Fuente Marcos C., Moni Bidin C., Carraro G., Costa E., 2013, MNRAS, 434, 194
De Silva G. M., Sneden C., Paulson D. B., Asplund M., Bland-Hawthorn J., Bessell M. S., Freeman K. C., 2006, AJ, 131, 455
De Silva G. M., Freeman K. C., Asplund M., Bland-Hawthorn J., Bessell M. S., Collet R., 2007, AJ, 133, 1161
de Silva G. M., Freeman K. C., Bland-Hawthorn J., Asplund M., Williams M., Holmberg J., 2011, MNRAS, 415, 563
De Silva G. M. et al., 2015, MNRAS, 449, 2604
Dehnen W., 1998, AJ, 115, 2384
Dias W. S., Alessi B. S., Moitinho A., Lépine J. R. D., 2002, A&A, 389, 871
Dias W. S., Alessi B. S., Moitinho A., Lepine J. R. D., 2014, VizieR Online Data Catalog
Dias W. S., Monteiro H., Assafin M., 2018, MNRAS, 478, 5184
Dreyer J. L. E., 1888, Mem. R. Astron. Soc., 49, 1
Eggen O. J., 1996, AJ, 111, 1615
Freeman K., Bland-Hawthorn J., 2002, ARA&A, 40, 487
Fregeau J. M., Ivanova N., Rasio F. A., 2009, ApJ, 707, 1533
Fujii M. S., Baba J., 2012, MNRAS, 427, L16
Gaia Collaboration, 2018a, preprint (arXiv:1804.09365)
Gaia Collaboration, 2018b, preprint (arXiv:1804.09378)
Gieles M., Bastian N., 2008, A&A, 482, 165
Gieles M., Athanassoula E., Portegies Zwart S. F., 2007, MNRAS, 376, 809
Gustafsson B., Church R. P., Davies M. B., Rickman H., 2016, A&A, 593, A85
Han E., Curtis J. L., Wright J. T., 2016, AJ, 152, 7
Hurley J. R., Aarseth S. J., Shara M. M., 2007, ApJ, 665, 707
Kereš D., Katz N., Weinberg D. H., Davé R., 2005, MNRAS, 363, 2
Kharchenko N. V., Piskunov A. E., Schilbach E., Röser S., Scholz R.-D., 2012, A&A, 543, A156
Kharchenko N. V., Piskunov A. E., Schilbach E., Röser S., Scholz R. D., 2013, A&A, 558
King I., 1962, AJ, 67, 471
Koposov S. E., Belokurov V., Torrealba G., 2017, MNRAS, 470, 2702
Kos J. et al., 2018, MNRAS, 473, 4612
Krumholz M. R., 2014, Phys. Rep., 539, 49
Marigo P. et al., 2017, ApJ, 835, 77
Martell S. L. et al., 2017, MNRAS, 465, 3203
Martinez-Medina L. A., Pichardo B., Moreno E., Peimbert A., Velazquez H., 2016, ApJ, 817, L3
Martinez-Medina L. A., Pichardo B., Peimbert A., Moreno E., 2017, ApJ, 834, 58

Miglio A. et al., 2012, MNRAS, 419, 2077
Odenkirchen M., Soubiran C., 2002, A&A, 383, 163
Pavani D. B., Bica E., Dutra C. M., Dottori H., Santiago B. X., Carranza G., Díaz R. J., 2001, A&A, 374, 554
Piskunov N., Valenti J. A., 2017, A&A, 597, A16
Salaris M., Chieffi A., Straniero O., 1993, ApJ, 414, 580
Sancisi R., Fraternali F., Oosterloo T., van der Hulst T., 2008, A&AR, 15, 189
Schmeja S., Kharchenko N. V., Piskunov A. E., Röser S., Schilbach E., Froebrich D., Scholz R.-D., 2014, A&A, 568, A51
Sestito P., Randich S., Bragaglia A., 2007, A&A, 465, 185
Skrutskie M. F. et al., 2006, AJ, 131, 1163
Stryker L. L., 1993, PASP, 105, 1081
Torrealba G., Belokurov V., Koposov S. E., 2018, preprint (arXiv:1805.06473)
Valenti J. A., Piskunov N., 1996, A&AS, 118, 595
Zwitter T. et al., 2018, preprint (arXiv:1804.06344)

APPENDIX A: LITERATURE MEMBERS FOR NGC 1252, NGC 6994, NGC 7772, AND NGC 7826

Tables A1–A4 list members given in the literature for four disproved clusters. Only stars we were able to cross-match with *Gaia* DR2 are listed. These stars are clearly not real members, but we use them to rest our case in Fig. 3. We also show HR diagrams using literature members and *Gaia* DR2 magnitudes. The HR diagrams do not resemble the diagrams for NGC 1901 or diagrams of other clusters explored with *Gaia* data in the literature (Cantat-Gaudin et al. 2018; Gaia Collaboration 2018b)

Table A1. Coordinates, proper motions, parallax, and radial velocity (where known) of NGC 1252 members from the literature. Not a single pair of stars can be found with matching parameters. Between all four sources the magnitudes of the stars extend from $V = 6.62$ to $V = 17.97$.

α °	δ °	$\mu_\alpha \cos(\delta)$ mas yr^{-1}	μ_δ mas yr^{-1}	ϖ mas	v_r km s^{-1}
		Members[a] in Kharchenko et al. (2013)			
47.4215	−57.6347	−0.03 ± 0.05	4.90 ± 0.04	0.95 ± 0.03	0.5 ± 0.6[b]
47.6764	−57.7014	−2.96 ± 0.03	15.57 ± 0.03	3.20 ± 0.02	
47.2933	−57.7678	−1.07 ± 0.06	−13.19 ± 0.05	1.08 ± 0.03	
48.0644	−57.6689	−4.70 ± 0.05	3.90 ± 0.05	1.39 ± 0.03	
47.7155	−57.6683	1.57 ± 0.05	−1.88 ± 0.04	0.61 ± 0.03	
47.9065	−57.5849	9.76 ± 0.15	3.23 ± 0.14	1.26 ± 0.07	
48.0170	−57.7205	2.12 ± 0.05	9.79 ± 0.04	0.98 ± 0.02	31.4 ± 0.3[c]
47.3650	−57.6324	−3.59 ± 0.10	12.80 ± 0.09	1.72 ± 0.05	
47.7089	−57.7856	0.04 ± 0.05	6.32 ± 0.04	1.63 ± 0.03	20.3 ± 0.8[b]
47.3982	−57.8135	6.42 ± 0.04	4.39 ± 0.03	0.76 ± 0.02	
47.9903	−57.6525	4.39 ± 0.14	9.04 ± 0.14	1.49 ± 0.07	
		Members in de la Fuente Marcos et al. (2013)			
47.6605	−57.7887	6.44 ± 0.05	7.61 ± 0.04	1.50 ± 0.02	−4.4 ± 1.1[b]
47.7356	−57.7966	5.55 ± 0.04	11.25 ± 0.03	1.09 ± 0.02	5.3 ± 0.2[c]
47.7498	−57.6912	9.95 ± 0.08	9.81 ± 0.07	0.85 ± 0.05	
47.4953	−57.7548	3.06 ± 0.10	10.20 ± 0.09	0.66 ± 0.05	
47.6336	−57.6454	3.49 ± 0.05	5.74 ± 0.05	0.81 ± 0.03	
47.9003	−57.6730	13.01 ± 0.03	6.05 ± 0.03	2.26 ± 0.02	
48.0170	−57.7205	2.12 ± 0.05	9.79 ± 0.04	0.98 ± 0.02	31.4 ± 0.3[c]
48.0104	−57.6817	5.09 ± 0.07	−0.90 ± 0.07	0.25 ± 0.04	
		Members in Pavani et al. (2001)			
47.7089	−57.7856	0.04 ± 0.05	6.32 ± 0.04	1.63 ± 0.03	20.3 ± 0.8[b]
47.6868	−57.7234	−21.39 ± 0.04	−44.09 ± 0.04	1.88 ± 0.02	20.1 ± 1.5[b]
47.7680	−57.7731	−17.57 ± 0.05	−18.16 ± 0.05	2.05 ± 0.03	
47.7356	−57.7966	5.55 ± 0.04	11.25 ± 0.03	1.09 ± 0.02	5.3 ± 0.2[c]
47.7498	−57.7446	31.21 ± 0.03	17.01 ± 0.03	1.77 ± 0.02	43.3 ± 4.4[b]
47.6764	−57.7014	−2.96 ± 0.03	15.57 ± 0.03	3.20 ± 0.02	
47.7083	−57.7021	4.05 ± 0.07	−69.89 ± 0.06	11.87 ± 0.04	54.0 ± 0.3[b]
		Members in Bouchet & The (1983)			
47.7083	−57.7021	4.05 ± 0.07	−69.89 ± 0.06	11.87 ± 0.04	54.0 ± 0.3[b]
48.1091	−57.7038	35.61 ± 0.04	1.30 ± 0.04	1.73 ± 0.02	50.8 ± 0.2[b]
48.2607	−57.8339	1.19 ± 0.07	−4.57 ± 0.08	1.08 ± 0.05	
48.2768	−57.6225	5.54 ± 0.05	17.82 ± 0.06	4.28 ± 0.03	30.8 ± 0.5[b]
48.2507	−57.5659	16.81 ± 0.04	4.41 ± 0.04	1.09 ± 0.02	30.8 ± 0.5[b]
48.0351	−57.5712	43.18 ± 0.06	15.34 ± 0.06	3.25 ± 0.03	7.6 ± 0.3[b]
47.9307	−57.5136	−5.85 ± 0.04	8.20 ± 0.04	2.12 ± 0.02	19.5 ± 0.2[b]
48.1921	−57.3504	−5.42 ± 0.06	3.69 ± 0.06	4.00 ± 0.03	−12.6 ± 0.5[b]
47.7845	−57.1932	−3.39 ± 0.09	−26.14 ± 0.10	4.86 ± 0.05	7.0 ± 0.5[b]
47.8202	−57.1590	19.11 ± 0.24	19.46 ± 0.23	1.77 ± 0.13	4.3 ± 0.3[b]
47.9257	−56.9778	−8.18 ± 0.04	−7.17 ± 0.04	1.82 ± 0.02	13.3 ± 0.2[b]
47.0998	−57.0100	14.40 ± 0.04	−13.60 ± 0.05	2.62 ± 0.03	5.6 ± 0.2[b]
48.7182	−57.8377	−6.38 ± 0.08	−15.96 ± 0.08	2.82 ± 0.05	105.3 ± 0.3[b]

[a]Only members with probability >0.8.
[b]v_r from *Gaia* DR2.
[c]v_r from GALAH.

Table A2. Coordinates, proper motions, parallax, and radial velocity (where known) of NGC 6994 members from the literature. Not a single pair of stars can be found with matching parameters. The magnitudes of the stars extend from $V = 10.35$ to $V = 19.53$.

α $^\circ$	δ $^\circ$	$\mu_\alpha \cos(\delta)$ mas yr^{-1}	μ_δ mas yr^{-1}	ϖ mas	v_r km s^{-1}
		Members in Bassino et al. (2000)			
314.7366	−12.6418	7.33 ± 0.07	−15.55 ± 0.05	1.41 ± 0.04	−26.2 ± 0.2[a]
314.7401	−12.6294	18.41 ± 0.07	−7.72 ± 0.06	2.66 ± 0.05	−53.1 ± 0.7[a]
314.7283	−12.6345	2.05 ± 0.09	−10.80 ± 0.07	3.11 ± 0.06	−8.5 ± 0.6[a]
314.7222	−12.6318	4.61 ± 0.07	−7.03 ± 0.05	1.52 ± 0.04	−20.8 ± 0.6[a]
314.8046	−12.6706	−21.38 ± 0.05	−9.39 ± 0.03	1.18 ± 0.03	
314.7781	−12.5914	3.50 ± 0.05	−6.02 ± 0.03	0.80 ± 0.03	−11.6 ± 0.1[b]
314.7776	−12.5777	−11.40 ± 0.07	1.19 ± 0.05	1.91 ± 0.05	
314.7423	−12.5768	−4.60 ± 0.04	−5.57 ± 0.03	0.83 ± 0.03	
314.7237	−12.5765	−4.16 ± 0.04	−6.62 ± 0.03	0.33 ± 0.03	51.5 ± 0.1[b]
314.7378	−12.5785	−5.53 ± 0.35	2.55 ± 0.23	1.78 ± 0.23	
314.7487	−12.6955	16.82 ± 0.07	7.75 ± 0.04	1.43 ± 0.04	−28.2 ± 1.6[a]

[a] v_r from *Gaia* DR2.
[b] v_r from GALAH.

Table A3. Coordinates, proper motions, parallax, and radial velocity (where known) of NGC 7772 members from the literature. Not a single pair of stars can be found with matching parameters. Between both sources the magnitudes of the stars extend from $V = 11.08$ to $V = 18.00$.

α $^\circ$	δ $^\circ$	$\mu_\alpha \cos(\delta)$ mas yr^{-1}	μ_δ mas yr^{-1}	ϖ mas	v_r km s^{-1}
		Members[a] in Kharchenko et al. (2013)			
357.9917	16.2920	17.13 ± 0.05	−8.65 ± 0.02	1.39 ± 0.03	
357.8054	16.1146	6.94 ± 0.34	−2.56 ± 0.14	1.30 ± 0.16	
357.5001	16.1331	12.52 ± 0.09	−10.44 ± 0.04	2.77 ± 0.04	22.7 ± 1.7[b]
358.2582	16.4424	18.28 ± 0.13	−14.25 ± 0.06	1.03 ± 0.07	
357.9434	16.2490	12.45 ± 0.05	−7.38 ± 0.02	1.88 ± 0.03	
357.9288	16.2352	7.30 ± 0.08	−8.65 ± 0.04	0.52 ± 0.04	22.1 ± 0.3[b]
357.9052	15.9786	11.59 ± 0.10	−7.66 ± 0.04	1.05 ± 0.05	
358.0828	16.2812	10.42 ± 0.30	−6.91 ± 0.18	1.53 ± 0.15	
357.9428	16.2398	12.50 ± 0.07	−7.25 ± 0.04	1.95 ± 0.04	−63.4 ± 0.1[c]
358.3233	16.0572	16.19 ± 0.09	−9.59 ± 0.04	1.03 ± 0.05	
		Members in Carraro (2002)			
357.9428	16.2398	12.50 ± 0.07	−7.25 ± 0.04	1.95 ± 0.04	−63.4 ± 0.1[c]
357.9690	16.1878	6.75 ± 0.16	−38.26 ± 0.08	5.48 ± 0.09	−20.1 ± 1.2[b]
357.9129	16.3036	−16.76 ± 0.06	−31.33 ± 0.03	2.04 ± 0.03	
357.9506	16.2513	8.65 ± 0.06	−10.52 ± 0.03	1.02 ± 0.03	−69.9 ± 1.3[b]
357.9434	16.2490	12.45 ± 0.05	−7.38 ± 0.02	1.88 ± 0.03	
357.8977	16.2136	−6.48 ± 0.05	−18.50 ± 0.02	0.64 ± 0.03	
357.9503	16.2333	0.52 ± 0.05	−2.54 ± 0.03	2.34 ± 0.03	18.8 ± 0.2[c]
357.9917	16.2920	17.13 ± 0.05	−8.65 ± 0.02	1.39 ± 0.03	
357.9367	16.2454	12.56 ± 0.05	5.86 ± 0.03	1.50 ± 0.03	
357.9538	16.1833	−4.48 ± 0.05	−6.55 ± 0.03	1.59 ± 0.03	−37.2 ± 0.1[c]
357.9056	16.3006	2.74 ± 0.08	0.49 ± 0.04	0.48 ± 0.04	

[a] Only members with probability >0.8.
[b] v_r from *Gaia* DR2.
[c] v_r from GALAH.

Table A4. Coordinates, proper motions, parallax, and radial velocity (where known) of NGC 7826 members from the literature. Not a single pair of stars can be found with matching parameters. The magnitudes of the stars extend from $V = 9.72$ to $V = 16.67$.

α °	δ °	$\mu_\alpha \cos(\delta)$ mas yr^{-1}	μ_δ mas yr^{-1}	ϖ mas	v_r km s^{-1}
		Members[a] in Dias et al. (2002, 2014)			
1.3897	−20.8588	12.26 ± 0.12	2.83 ± 0.07	0.72 ± 0.07	
1.1267	−20.6970	46.70 ± 0.09	−5.49 ± 0.06	3.22 ± 0.06	−1.1 ± 0.2[b]
1.2085	−20.6567	25.99 ± 0.06	−11.67 ± 0.04	1.30 ± 0.03	
1.2711	−20.6347	15.25 ± 0.07	−8.40 ± 0.05	0.36 ± 0.04	77.3 ± 0.1[c]
1.2949	−20.7413	14.65 ± 0.10	1.17 ± 0.06	1.18 ± 0.05	
1.2976	−20.6020	19.74 ± 0.05	6.47 ± 0.03	0.79 ± 0.03	−17.8 ± 0.1[c]
1.3595	−20.7226	38.34 ± 0.12	5.27 ± 0.06	3.39 ± 0.05	16.3 ± 0.7[b]
1.3745	−20.6056	27.03 ± 0.07	−5.63 ± 0.04	3.53 ± 0.04	−2.9 ± 0.1[c]
1.4658	−20.7048	16.05 ± 0.05	−5.44 ± 0.04	0.92 ± 0.04	
1.2480	−20.5623	18.41 ± 0.07	−8.65 ± 0.05	1.99 ± 0.04	12.9 ± 1.1[b]
1.4210	−20.5883	12.84 ± 0.08	1.43 ± 0.04	2.54 ± 0.04	

[a]Only members with probability >0.9.
[b]v_r from *Gaia* DR2.
[c]v_r from GALAH.

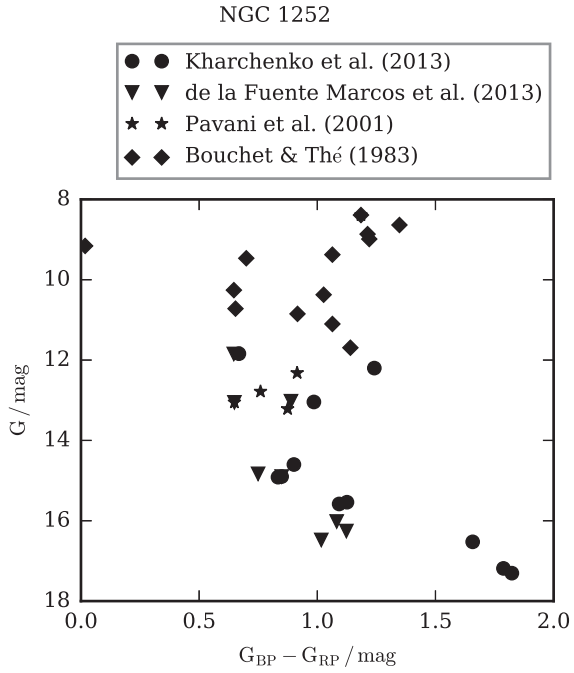

Figure A1. HR diagram of stars in Table A1.

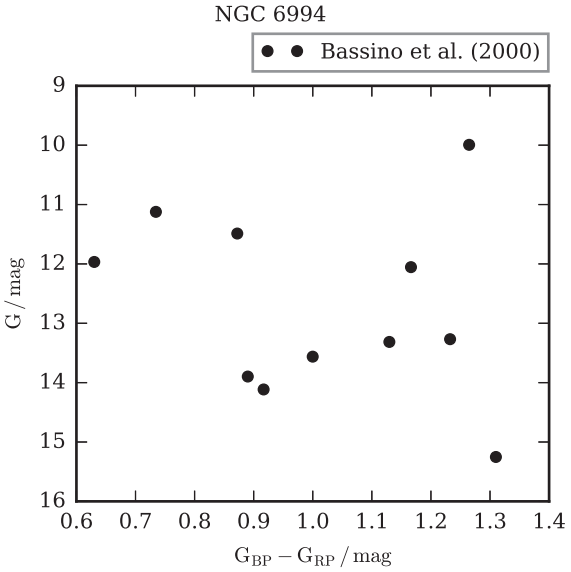

Figure A2. HR diagram of stars in Table A2.

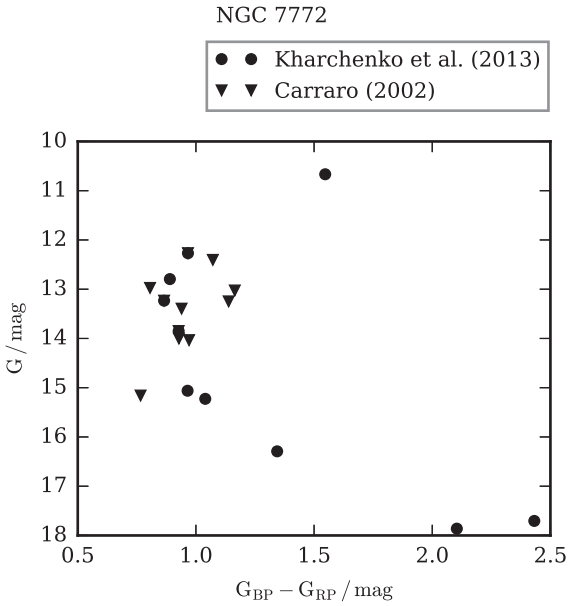

Figure A3. HR diagram of stars in Table A3.

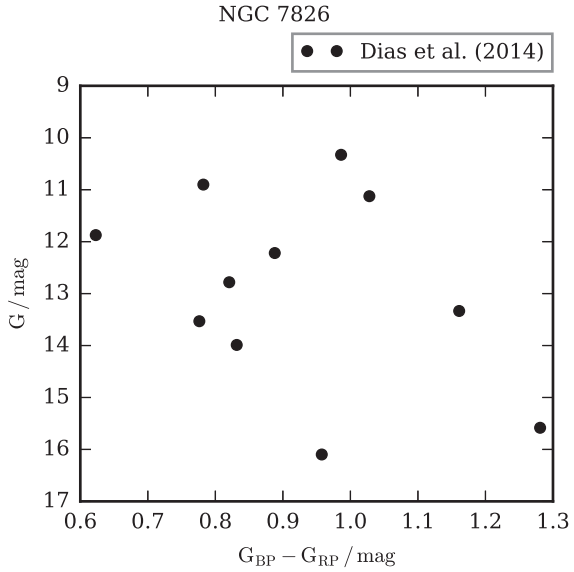

Figure A4. HR diagram of stars in Table A4.

APPENDIX B: LIST OF PROBABLE NGC 1901 MEMBERS

In Table B1 we list the most probable NGC 1901 members. Note that only stars in the *Gaia* DR2 are included. Fig. B1 shows the position of the most probable members on the sky.

Table B1. List of most probable NGC 1901 members ordered by probability. Probability P_{5D} is given to all stars in *Gaia* DR2 with known position, proper motions, and parallax. The uncertainty of all measurements is properly taken into account. Stars with known radial velocity are given another probability (P_{6D}) based on their radial velocity. Stars with GALAH radial velocities are marked with an asterisk. r is the distance from the cluster centre. Possible binaries have been identified from the GALAH spectra for stars with GALAH v_r only.

Gaia DR2 source id	α °	δ °	r °	$\mu_\alpha \cos(\delta)$ mas yr^{-1}	μ_δ mas yr^{-1}	ϖ mas	G mag	v_r km s^{-1}	P_{5D}	P_{6D}	Possible binary
4658338537313572096	79.5799	−68.4403	0.104	1.490 ± 0.042	12.736 ± 0.056	2.368 ± 0.026	12.48	1.43 ± 0.06*	0.983	0.983	
4658335518014051712	79.6781	−68.4590	0.136	1.666 ± 0.042	12.592 ± 0.057	2.324 ± 0.026	11.49	3.01 ± 0.11*	0.977	0.942	√
4658765564465430272	79.3346	−68.1278	0.222	1.727 ± 0.035	12.684 ± 0.052	2.333 ± 0.021	14.78		0.972		
4658340053499327360	79.3992	−68.3630	0.040	1.792 ± 0.042	12.825 ± 0.053	2.388 ± 0.027	10.81	−11.58 ± 6.40*	0.966	0.125	
4658338747829382528	79.5499	−68.4267	0.088	1.425 ± 0.063	12.620 ± 0.075	2.340 ± 0.032	10.33	−0.49 ± 3.88*	0.963	0.926	
4658384751164454016	79.1349	−68.4621	0.178	1.558 ± 0.033	12.617 ± 0.042	2.360 ± 0.018	13.52		0.954		
4658384755525236864	79.1097	−68.4584	0.182	1.703 ± 0.049	12.647 ± 0.059	2.357 ± 0.031	12.72	6.07 ± 7.08	0.946	0.715	
4658333422070733312	79.7205	−68.5703	0.243	1.652 ± 0.045	12.869 ± 0.058	2.323 ± 0.028	10.37	−4.09 ± 0.82*	0.936	0.654	
4658726218241467008	79.6766	−68.0353	0.314	1.819 ± 0.054	12.558 ± 0.060	2.361 ± 0.032	10.40		0.929		
4658714677689040640	79.5087	−68.3554	0.015	1.709 ± 0.044	12.942 ± 0.065	2.331 ± 0.026	9.21		0.928		
4658765736264109312	79.2926	−68.1346	0.220	1.700 ± 0.047	12.537 ± 0.059	2.282 ± 0.025	9.74	0.95 ± 4.90*	0.918	0.917	
4658388260218178048	78.9761	−68.2895	0.197	1.671 ± 0.037	12.729 ± 0.050	2.398 ± 0.023	11.98	54.53 ± 0.21*	0.905	0.000	√
4658378570770738944	79.2189	−68.5038	0.190	1.404 ± 0.085	12.759 ± 0.089	2.367 ± 0.044	16.14		0.904		
4658329298899347328	79.1740	−68.6263	0.307	1.655 ± 0.055	12.778 ± 0.065	2.290 ± 0.033	10.21		0.896		
4658328680424119552	79.1905	−68.6844	0.360	1.834 ± 0.035	12.825 ± 0.041	2.391 ± 0.022	14.23		0.896		
4658766114221175040	79.1298	−68.1230	0.257	1.888 ± 0.044	12.597 ± 0.068	2.367 ± 0.024	11.34	1.61 ± 1.79*	0.894	0.893	√
4658751030294843776	79.5615	−67.9204	0.422	1.749 ± 0.085	12.950 ± 0.107	2.382 ± 0.048	15.04		0.806		
4658349364997640064	78.9891	−68.8448	0.535	1.885 ± 0.033	12.586 ± 0.032	2.309 ± 0.021	13.02		0.797		
4658709970404987904	79.9753	−68.4676	0.218	1.453 ± 0.060	12.870 ± 0.084	2.434 ± 0.040	15.89		0.778		
4658760822820870144	79.8711	−67.7024	0.655	1.586 ± 0.049	12.884 ± 0.054	2.409 ± 0.022	14.73		0.770		
4658733335028239232	80.2483	−68.1295	0.352	1.458 ± 0.030	12.684 ± 0.030	2.430 ± 0.017	13.04		0.765		
4658764499313514112	79.1826	−68.1872	0.192	1.911 ± 0.049	12.461 ± 0.069	2.443 ± 0.030	9.03		0.752		
4658748109717269120	80.1748	−67.9189	0.494	1.447 ± 0.074	12.760 ± 0.080	2.395 ± 0.044	16.20		0.748		
4658286069991771392	80.1431	−68.9948	0.695	1.648 ± 0.044	12.546 ± 0.049	2.349 ± 0.022	12.56	−1.51 ± 1.00	0.738	0.669	
4658732265555421952	80.3665	−68.1686	0.368	1.416 ± 0.045	12.418 ± 0.048	2.375 ± 0.025	12.39	13.68 ± 0.11*	0.722	0.109	
4658383033177728512	78.8183	−68.3973	0.254	1.783 ± 0.117	12.413 ± 0.143	2.330 ± 0.070	16.77		0.705		
4658764877270576000	79.0623	−68.1334	0.262	1.703 ± 0.053	13.032 ± 0.072	2.426 ± 0.032	8.79		0.702		
4658332631796592768	79.7948	−68.5810	0.264	1.478 ± 0.051	12.252 ± 0.066	2.385 ± 0.031	9.83		0.678		
4658761887972710144	79.6859	−67.6594	0.687	1.438 ± 0.069	12.987 ± 0.070	2.285 ± 0.029	10.41	1.87 ± 0.57*	0.675	0.673	√
4658854831036783232	80.1141	−67.5098	0.865	1.472 ± 0.059	12.744 ± 0.075	2.327 ± 0.032	10.52	−11.26 ± 1.63*	0.661	0.094	√
4658854002110866688	80.1928	−67.5869	0.800	1.436 ± 0.056	12.488 ± 0.055	2.348 ± 0.026	12.79	3.71 ± 3.59	0.660	0.614	
4658693507772922624	80.4737	−68.6163	0.453	1.496 ± 0.046	12.385 ± 0.053	2.307 ± 0.030	10.21	−1.14 ± 0.53	0.648	0.602	
4658191172772162944	79.5185	−69.3746	1.033	1.596 ± 0.042	12.702 ± 0.057	2.394 ± 0.027	14.90		0.646		
4658758963072125312	79.8855	−67.7579	0.603	1.624 ± 0.052	13.071 ± 0.049	2.357 ± 0.026	12.34	4.11 ± 0.48*	0.644	0.585	√
4658779342721084160	78.9703	−67.8583	0.521	1.641 ± 0.160	12.620 ± 0.201	2.266 ± 0.082	17.35		0.629		
4658806005880090368	78.9761	−67.6454	0.723	1.817 ± 0.075	12.884 ± 0.094	2.433 ± 0.043	15.14		0.628		
4658198766214889856	79.0002	−69.1475	0.825	1.663 ± 0.060	12.347 ± 0.067	2.382 ± 0.034	15.76		0.625		
4658286933330473600	79.8546	−68.9528	0.625	1.621 ± 0.033	12.260 ± 0.047	2.324 ± 0.017	14.00		0.618		
4658385305280833152	79.1563	−68.4135	0.142	1.372 ± 0.054	13.111 ± 0.073	2.354 ± 0.037	13.53		0.610		
4658275659025982592	79.8104	−69.2550	0.920	1.367 ± 0.038	12.346 ± 0.062	2.364 ± 0.025	14.52		0.580		
4658765736264108800	79.2927	−68.1340	0.220	1.372 ± 0.162	12.756 ± 0.112	2.234 ± 0.061	12.85		0.572		

Table B1 – *continued*

Gaia DR2 source id	α $^\circ$	δ $^\circ$	r $^\circ$	$\mu_\alpha \cos(\delta)$ mas yr^{-1}	μ_δ mas yr^{-1}	ϖ mas	G mag	v_r km s^{-1}	P_{5D}	P_{6D}	Possible binary
4658293083726796928	79.2046	−69.0403	0.706	1.731 ± 0.128	12.339 ± 0.159	2.344 ± 0.088	16.96		0.556		
4658709553769767424	80.3100	−68.1705	0.349	1.666 ± 0.154	12.974 ± 0.178	2.329 ± 0.094	17.56		0.551		
4658812053194570240	79.1862	−67.5435	0.807	1.636 ± 0.058	12.858 ± 0.070	2.237 ± 0.038	8.80		0.549		
4658743608590786432	80.6294	−67.8497	0.650	1.407 ± 0.061	12.880 ± 0.058	2.412 ± 0.030	12.16	1.82 ± 0.14*	0.545	0.543	√
4658785493114963328	78.3230	−67.9287	0.600	1.871 ± 0.081	12.932 ± 0.067	2.328 ± 0.060	10.51	1.53 ± 0.53	0.517	0.516	
4658336548806471936	79.4965	−68.5243	0.182	1.578 ± 0.062	12.169 ± 0.081	2.310 ± 0.035	10.41	−0.96 ± 0.87*	0.516	0.485	
4658730070853284608	80.7501	−68.1758	0.495	1.269 ± 0.032	12.647 ± 0.035	2.367 ± 0.018	14.24		0.509		
4658377810497066368	78.8767	−68.5252	0.290	1.717 ± 0.142	12.960 ± 0.186	2.257 ± 0.095	17.61		0.502		
4658360458826656128	78.3023	−68.7202	0.576	1.624 ± 0.048	13.046 ± 0.058	2.347 ± 0.028	12.35	7.36 ± 3.49	0.491	0.312	
4658727528232702976	80.8333	−68.2937	0.499	1.316 ± 0.038	12.636 ± 0.045	2.272 ± 0.023	11.23	0.98 ± 0.09*	0.484	0.483	
4658737423838030080	80.7492	−68.0642	0.544	1.417 ± 0.061	12.714 ± 0.063	2.252 ± 0.033	9.66		0.481		
4658337820116699648	79.3460	−68.4719	0.140	1.348 ± 0.062	12.174 ± 0.080	2.299 ± 0.036	9.13		0.481		
4658188350951010560	78.9303	−69.3897	1.067	1.831 ± 0.045	12.295 ± 0.055	2.309 ± 0.026	15.28		0.463		
4658162241856515712	78.7408	−69.5461	1.234	1.636 ± 0.055	12.438 ± 0.065	2.368 ± 0.031	15.65		0.455		
4658515700465243392	80.8487	−68.3891	0.503	1.281 ± 0.038	12.411 ± 0.048	2.306 ± 0.024	11.87	1.63 ± 0.39*	0.454	0.453	√
4658276728485892224	80.0309	−69.2272	0.907	1.584 ± 0.074	12.259 ± 0.115	2.277 ± 0.043	16.15		0.444		
4658540989235266176	81.1009	−68.2522	0.602	1.425 ± 0.025	12.754 ± 0.029	2.358 ± 0.016	13.07		0.438		
4658833321873098368	80.9618	−67.8727	0.722	1.375 ± 0.039	12.874 ± 0.038	2.411 ± 0.019	14.04		0.427		
4658548337881959424	81.0902	−68.1410	0.626	1.523 ± 0.050	12.747 ± 0.053	2.430 ± 0.027	11.91	0.82 ± 0.02*	0.411	0.410	√
4658316173421984128	80.3508	−68.7060	0.481	1.281 ± 0.191	12.454 ± 0.233	2.310 ± 0.108	18.02		0.398		
4658797244146158976	78.2421	−67.6328	0.849	1.813 ± 0.139	12.513 ± 0.168	2.330 ± 0.092	17.56		0.391		
4658794838964513792	78.2221	−67.7434	0.764	2.022 ± 0.069	12.619 ± 0.069	2.279 ± 0.037	9.74	−3.73 ± 6.32*	0.387	0.283	
4658874381762648320	80.6001	−67.3468	1.080	1.287 ± 0.033	12.937 ± 0.039	2.394 ± 0.018	14.27		0.378		
4658380799796398464	78.8235	−68.4930	0.288	1.810 ± 0.270	12.475 ± 0.367	2.360 ± 0.163	18.33		0.372		
4658265041838712320	77.9610	−68.8592	0.761	1.935 ± 0.080	12.489 ± 0.082	2.367 ± 0.043	15.97		0.371		
4658515631745778944	80.8804	−68.3981	0.516	1.180 ± 0.069	12.752 ± 0.087	2.380 ± 0.043	16.06		0.339		
4658256902970784000	77.8433	−68.9710	0.869	1.362 ± 0.055	12.517 ± 0.052	2.404 ± 0.029	11.29	−0.37 ± 0.60*	0.334	0.323	√
4658375031727651584	77.8276	−68.3802	0.614	2.014 ± 0.053	12.881 ± 0.060	2.303 ± 0.030	11.21	6.10 ± 1.39	0.319	0.240	
4658395230881878272	78.2224	−68.3594	0.468	2.121 ± 0.031	12.961 ± 0.038	2.406 ± 0.016	13.16		0.317		
4658818787703876096	78.7098	−67.5983	0.799	1.966 ± 0.024	12.194 ± 0.027	2.248 ± 0.014	13.09		0.311		

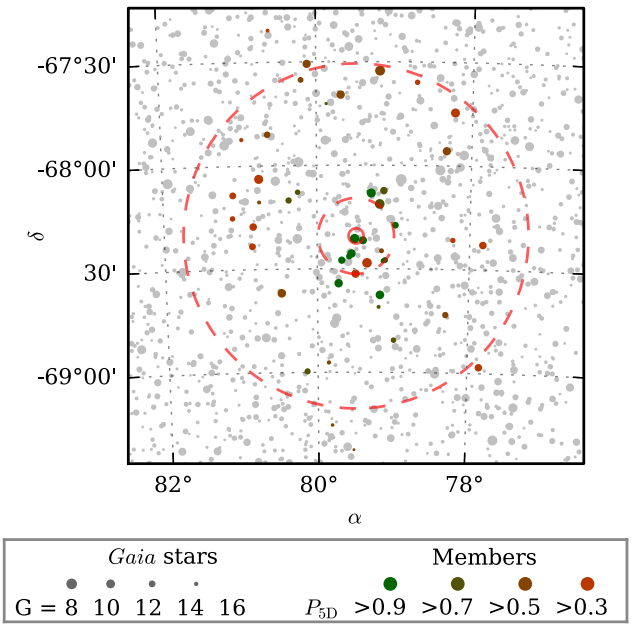

Figure B1. Positions of the most probable NGC 1901 members. All *Gaia* DR2 stars with $G < 16$ are plotted in grey and the members are plotted in colour. Radii r_0, r_1, and r_2 are marked with red circles.

APPENDIX C: ABUNDANCES

Temperatures, gravities, and abundances in Table C1 are calculated by SME (Valenti & Piskunov 1996; Piskunov & Valenti 2017). Some stars that might be binaries are used. For most members the precise stellar parameters and abundances cannot be computed, as the temperatures are too high.

Table C1. Effective temperature, gravity, and abundances for 19 elements in eight NGC 1901 stars.

Gaia DR2 source id	$T_{\rm eff}$	$\log g$	$\left[\frac{\rm Li}{\rm Fe}\right]$	$\left[\frac{\rm C}{\rm Fe}\right]$	$\left[\frac{\rm O}{\rm Fe}\right]$	$\left[\frac{\rm Na}{\rm Fe}\right]$	$\left[\frac{\rm Mg}{\rm Fe}\right]$	$\left[\frac{\rm Al}{\rm Fe}\right]$	$\left[\frac{\rm Si}{\rm Fe}\right]$	$\left[\frac{\rm K}{\rm Fe}\right]$	$\left[\frac{\rm Ca}{\rm Fe}\right]$	$\left[\frac{\rm Sc}{\rm Fe}\right]$	$\left[\frac{\rm Ti}{\rm Fe}\right]$	$\left[\frac{\rm Cr}{\rm Fe}\right]$	$\left[\frac{\rm Mn}{\rm Fe}\right]$	$\left[\frac{\rm Fe}{\rm H}\right]$	$\left[\frac{\rm Ni}{\rm Fe}\right]$	$\left[\frac{\rm Cu}{\rm Fe}\right]$	$\left[\frac{\rm Zn}{\rm Fe}\right]$	$\left[\frac{\rm Y}{\rm Fe}\right]$	$\left[\frac{\rm Ba}{\rm Fe}\right]$
	K	dex	dex	dex	dex	dex	dex	dex	dex	dex	dex	dex	dex	dex	dex	dex	dex	dex	dex	dex	dex
4658515700465243392	6265	4.17			0.03	0.04	0.09		0.14	0.13		0.18		−0.05	−0.12	−0.29			−0.11		0.47
4658727528232702976	6483	4.04		0.07	0.21	−0.02	0.02		0.21	0.14	0.10	0.12	0.05	0.06	−0.05	−0.29			−0.06	0.15	0.44
4658766114221175040	5840	4.40	1.85		0.06	−0.02	−0.05		0.11	0.03						−0.15		−0.11	0.10	0.05	0.94
4658338537313572096	5982	4.35	1.88		−0.03	−0.07	0.03		0.11	0.12	−0.10	0.05				−0.16		−0.09		0.07	0.44
4658743608590786432	6076	4.29	1.77		0.18	0.01	0.10		0.03	0.09	0.05	0.10	0.02	0.03	−0.03	−0.29		−0.13	−0.05	0.06	0.60
4658766114221175040	6596	4.12			0.08	0.04	0.09			0.11	0.23	0.17				−0.27			0.01		0.56
4658732265555421952	6008	4.34	2.14		0.09	−0.06	0.02	−0.13	0.03	0.11	0.09	0.08	−0.01	0.12	−0.07	−0.19	0.00	−0.06	0.05	0.28	0.48
4658548337881959424	6015	4.25			0.54	0.16	0.08		0.24	0.16					0.18	−0.45			0.04		0.79

This paper has been typeset from a TEX/LATEX file prepared by the author.